Metallophysics and Advanced Technologies
Металофіз. новітні технол.
Metallofiz. Noveishie Tekhnol.
2025, vol. 47, No. 3, pp. 271–285
https://doi.org/10.15407/mfint.47.03.0271
Reprints available directly from the publisher

PACS numbers: 06.60.Vz, 61.66.Dk, 61.72.Ff, 66.10.cg, 81.20.Vj, 81.70.Jb, 83.50.Uv

The Influence of the Size of the Brazing Gap on the Structure and Strength of Kovar Joints with Stainless Steel

S. V. Maksymova, P. V. Koval'chuk, and V. V. Voronov

E. O. Paton Electric Welding Institute, N.A.S. of Ukraine,
11 Kazymyr Malevych Str.,
UA-03150 Kyiv, Ukraine

Comprehensive studies of the influence of brazing gap widths (100, 50, 20 μm) on the structure and mechanical properties of brazed dissimilar joints between Kovar and stainless steel, utilizing Cu–Mn–4.5Co–2.5Fe filler metal during high-temperature vacuum brazing, are presented. X-ray microspectral analysis reveals a two-phase structure in the brazed seams, when Cu–Mn–Co–2.5Fe filler metal is employed. This structure consists of both the α-Cu phase forming the main zone of the brazed seam (with a 100 or 500 μm gap) and discrete grains of the γ-phase $(Fe_xMn_yCo_z)Me$. During brazing, mutual-diffusion processes occur at the interphase boundary between the liquid filler metal and the solid base metal. The filler metal becomes saturated with constituent components of the base metal—chromium, cobalt, and nickel—thus, influencing the chemical composition and mechanical properties of the brazed seam. Micro-x-ray spectral analysis indicates that reducing the gap from 100 to 20 μm increases the γ-phase $(Fe_xMn_yCo_z)Me$ content in the seam from 13.20% to 90.90%, while simultaneously decreasing the α-Cu phase from 86.83% to 9.10%. These structural changes positively affect the mechanical properties of the brazed dissimilar joints, leading to increased shear strength in Kovar–stainless steel overlap joints. With a gap size of 20 μm, the brazed samples exhibited failure primarily on the stainless steel (600 MPa).

Key words: copper–manganese–cobalt–iron filler metal, brazing gap, structure, strength, high-temperature vacuum brazing, solid solution.

Corresponding author: Svitlana Vasylivna Maksymova
E-mail: maksymova.svitlana15@ukr.net

Citation: S. V. Maksymova, P. V. Koval'chuk, and V. V. Voronov, The Influence of the Size of the Brazing Gap on the Structure and Strength of Kovar Joints with Stainless Steel, *Metallofiz. Noveishie Tekhnol.*, **47**, No. 3: 271–285 (2025). DOI: 10.15407/mfint.47.03.0271

Наведено результати комплексних досліджень впливу паяльного зазору (100, 50, 20 μm) за використання припою Cu–Mn–4,5Co–2,5Fe на структуру та механічні властивості паяних різнорідних з'єднань ковар–корозійнотривка криця за вакуумного високотемпературного лютування. Мікрорентґеноспектральною аналізою встановлено, що за застосування припою Cu–Mn–Co–2,5Fe у паяних швах формується двофазна структура, яку утворено первинною фазою — твердим розчином на основі системи Cu–Mn (α-Cu), який заповнює основну зону паяного шву (із зазором у 100, 50 мкм), і незначною кількістю окремих дискретних зерен γ-фази ($Fe_xMn_yCo_z$)*Me*. Встановлено, що під час процесу лютування перебігають взаємні дифузійні процеси на міжфазній межі між рідким припоєм і твердим основним металом. Припій насичується складовими компонентами основного металу: Хромом, Кобальтом і Ніклем, що впливає на хемічний склад металу паяного шва, відповідно, на механічні властивості паяних з'єднань. За результатами мікрорентґеноспектральної аналізи визначено, що зменшення зазору зі 100 до 20 μm приводить до збільшення кількости γ-фази ($Fe_xMn_yCo_z$)*Me* у шві з 13,20 до 90,90% і одночасного зменшення кількости α-Cu фази з 86,83 до 9,10%. Такі структурні особливості паяних різнорідних з'єднань позитивно впливають на їхні механічні властивості та сприяють збільшенню міцности на зріз напускних з'єднань ковар–корозійнотривка криця. За величини зазору у 20 мкм руйнування зразків відбувалося по основному металу — корозійнотривкій криці (600 МПа).

Ключові слова: припій Купрум–Манґан–Кобальт–Ферум, паяльний зазор, структура, міцність, високотемпературне вакуумне лютування, твердий розчин.

(Received 20 May, 2024; in final version, 1 February, 2025)

1. INTRODUCTION

The utilization of dissimilar material joints, such as Kovar with stainless steel, is becoming increasingly prevalent in the creation of responsible structures across various industries including electronics, energy, and automotive sectors [1–4]. Kovar is a precision iron-based alloy containing 29% nickel and 17% cobalt, which is characterized by a low coefficient of thermal expansion and is used in the production of individual brazed joints with glass, ceramics or other materials [5]. Stainless steel contains chromium, nickel, titanium or other alloying elements that increase its resistance to corrosion in various environments [6].

Several technological processes, including brazing, diffusion welding, electron beam, and laser welding, have been explored to fabricate Kovar joints with stainless steel [7–12]. Among these, brazing emerges as a promising and reliable method. Brazing facilitates the formation of interatomic bonds between materials by heating them to a temperature below the base metal melting point. With a suitably chosen filler

metal composition possessing a melting temperature range, it becomes possible to preserve the original structure and mechanical properties of the base metal [13].

By vacuum brazing, alongside temperature and holding time, the size of the brazing gap between the connecting parts represents a crucial parameter. It is well established that the structure formation in brazed seams and the resulting mechanical properties of brazed joints is closely linked to the size of the brazing gap [14–16].

This study aims to investigate the impact of gap size on the structure and mechanical properties of dissimilar Kovar-stainless steel joints obtained through vacuum high-temperature brazing, utilizing Cu–Mn–Co–Fe filler metal.

2. EXPERIMENTAL/THEORETICAL DETAILS

Experimental Cu–Mn–4.5Co–2.5Fe filler metal was produced by argon-arc melting using a non-fusible tungsten electrode on a cold copper substrate within a high-purity argon environment (argon volume fraction not less than 99.993%). To ensure uniform distribution of alloying elements throughout the ingot volume, the filler metal underwent fivefold remelting. For experimentation purposes, the filler metal was utilized in its cast state, boasting a melting temperature range of 917–957°C [17].

Base metal samples for mechanical testing (three samples per gap size) were crafted from precision alloy Kovar and stainless steel 12Kh18N10T, each measuring 80×15×2 (Fig. 1 and Table 1). The overlap size did not exceed the thickness of the brazed plates, which was 2 mm.

High-temperature brazing utilizing experimental filler metal was

TABLE 1. Chemical composition of Kovar (29NK) and steel 12Kh18N10T [18].

Grade	Chemical elements, wt. %									
	Fe	Ni	Co	C	Si	Mn	Cr	Ti	Al	Cu
Kovar	51.14–54.5	28.5–29.5	17–18	0.03	0.3	0.4	0.1	0.1	0.2	0.2
12Kh18N10T	67	9–1	–	0.12	0.8	2	17–19	0.4–1	–	0.3

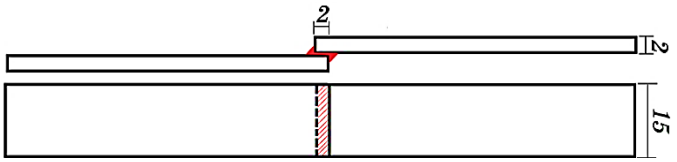

Fig. 1. Schematic representation of Kovar–stainless steel brazed joints.

conducted in a vacuum furnace (model SGV 2.4-2/15-I3) with radiation heating, featuring a working space rarefaction corresponds to 1.33×10^{-3} Pa. Heating was performed at a controlled rate not exceeding 18–20°C/min, while cooling within the temperature range of 1060 to 200°C maintained a rate of 10–15°C/min. Temperature measurement error was kept within ±5°C. The brazing temperature surpassed the liquidus temperature of the filler metal by 30°C, with a holding time at the brazing temperature set to 3 minutes. Prior to brazing, mechanical processing of the samples involved polishing with a 125 μm diamond tool and degreasing with B-70 gasoline followed by dehydration using technical alcohol. The cast-state filler metal (weighing 0.1–0.15 g) was positioned near the gap and secured using a contact welding machine. Gap sizes for the three batches of samples were maintained at 20 μm, 50 μm, and 100 μm, respectively. The samples were brazed without clamping or additional loading.

Post-brazing, samples composed of dissimilar materials were sectioned perpendicular to the seam, and microsections were prepared following standard procedures. Metallographic examinations and micro-x-ray spectral analyses were carried out using a TescanMira 3 LMU scanning electron microscope. The distribution of elements within separate phases was studied by localized micro-x-ray spectral analysis employing an Oxford Instruments X-max 80 mm^2 energy dispersive spectrometer. Microsections were observed without chemical etching, utilizing the reflected electron (BSE) mode, with measurement locality maintained within 1 μm. Mechanical properties of brazed joints were evaluated at room temperature utilizing a ZDM 10 Zwick-1488 testing machine. Percentage ratios of phases were determined through SEM image analysis using the ImageJ program, with an error margin of ±1.5%.

3. RESULTS AND DISCUSSION

During high-temperature vacuum brazing of Kovar flat samples with stainless steel using Cu–Mn–Co–2.5Fe filler metal, tight brazed seams are consistently achieved. The brazing gap size within the range of 20–100 μm does not impede the filler metal ability to wet both base materials and evenly spread over them. Notably, a well-formed direct and reverse fillet with negligible dimensions is observed (Fig. 2).

No defects such as erosion, unbrazing, cracks, or cavities were identified during visual inspection of the brazed joints. Remarkably, despite the base metal samples possessing varying coefficients of thermal linear expansion (Table 2), they maintained their geometric dimensions. This observation suggests the appropriate selection of the basic alloying system of the filler metal and hints at the potential relaxation of stresses between Kovar and stainless steel.

Thorough examinations of the structure of brazed joints (with a gap

TABLE 2. Coefficients of thermal linear expansion of stainless steel and forged steel [19, 20].

Temperature, °C	Coefficients of thermal linear expansion, 10^{-6}/°C	
	12Kh18H10T	Kovar
20	–	
100	16.6	5.86
200	17	5.20
300	17.2	5.13
350	–	4.89
400	17.5	5.06
450	–	5.25
500	17.9	6.15
600	18.2	7.80
700	18.6	9.12
800	18.9	10.31
900	19.3	11.26

size of 100 μm) using scanning electron microscopy in the reflected electron mode validated the superior quality formation of brazed seams (Fig. 3). It is worth noting that contrast in this mode is contingent upon the atomic number of the constituent elements within the brazed joint and obviates the need for chemical etching to discern the chemical composition of distinct phases.

The findings from local x-ray microspectral analysis confirmed a two-phase composition of the seam. The primary phase, constituting 86.83% of the total area of the seam, consists of a homogeneous Cu–Mn solid solution, incorporating trace amounts of nickel, iron, and cobalt (Fig. 3 and Table 3, spectrum 4).

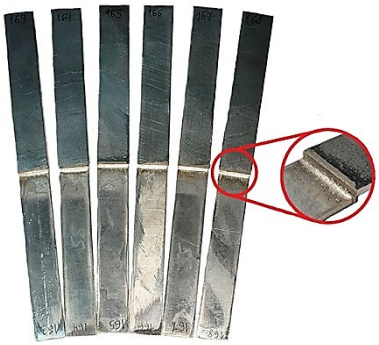

Fig. 2. Appearance of brazed samples.

TABLE 3. Chemical composition of separate phases in the Kovar–stainless steel brazed seam by 100 μm gap size.

No. spectrum	Chemical elements, wt.%							
	Si	Ti	Cr	Mn	Fe	Co	Ni	Cu
1	0.54	0.22	17.87	1.37	71.50	0.00	8.50	0.00
2	0.14	0.65	2.91	32.16	32.58	20.11	2.54	8.91
3	0.17	0.00	3.28	30.38	34.35	19.87	3.32	8.63
4	0.00	0.00	0.00	26.49	1.12	1.43	3.48	67.48
5	0.00	0.00	2.87	28.50	34.25	19.60	4.68	10.10
6	0.17	0.00	1.97	31.23	35.12	18.83	3.86	8.83
7	0.12	0.00	1.93	28.64	36.72	18.40	5.85	8.34
8	0.27	0.00	0.00	0.39	52.75	18.01	28.58	0.00

The second phase comprises discrete dark grains of an iron-based phase, which also incorporate other constituents from both the filler metal and the base metal (Table 3, spectrum 2, 3, 5, 6, and 7). The concentration of iron within these grains falls within the range of 32.58–36.72%. According to binary diagrams of metal systems, this compound likely corresponds to the γ phase $(Fe_xMn_yCo_z)Me$ [21]. Notably, with a gap size of 100 μm, this phase predominantly crystallizes near the seam's border with the base metal. In the central zone of the seam, its presence is minimal, except for isolated single grains of minor sizes ranging from 4 to 10 μm. These grains exhibit enrichment in iron, manganese, and cobalt, collectively occupying 13.17% of the seam area.

The results of electron beam scanning perpendicular to the seam corroborate previous findings and confirm the homogeneous distribution of manganese across the entire width of the brazed seam.

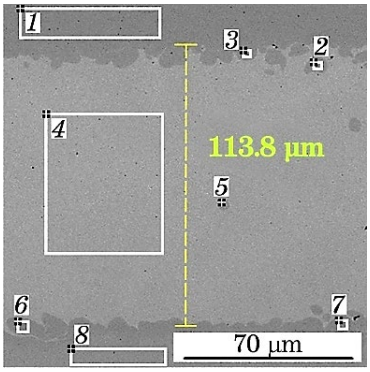

Fig. 3. Microstructure of a brazed dissimilar Kovar–stainless steel joint by 100 μm gap.

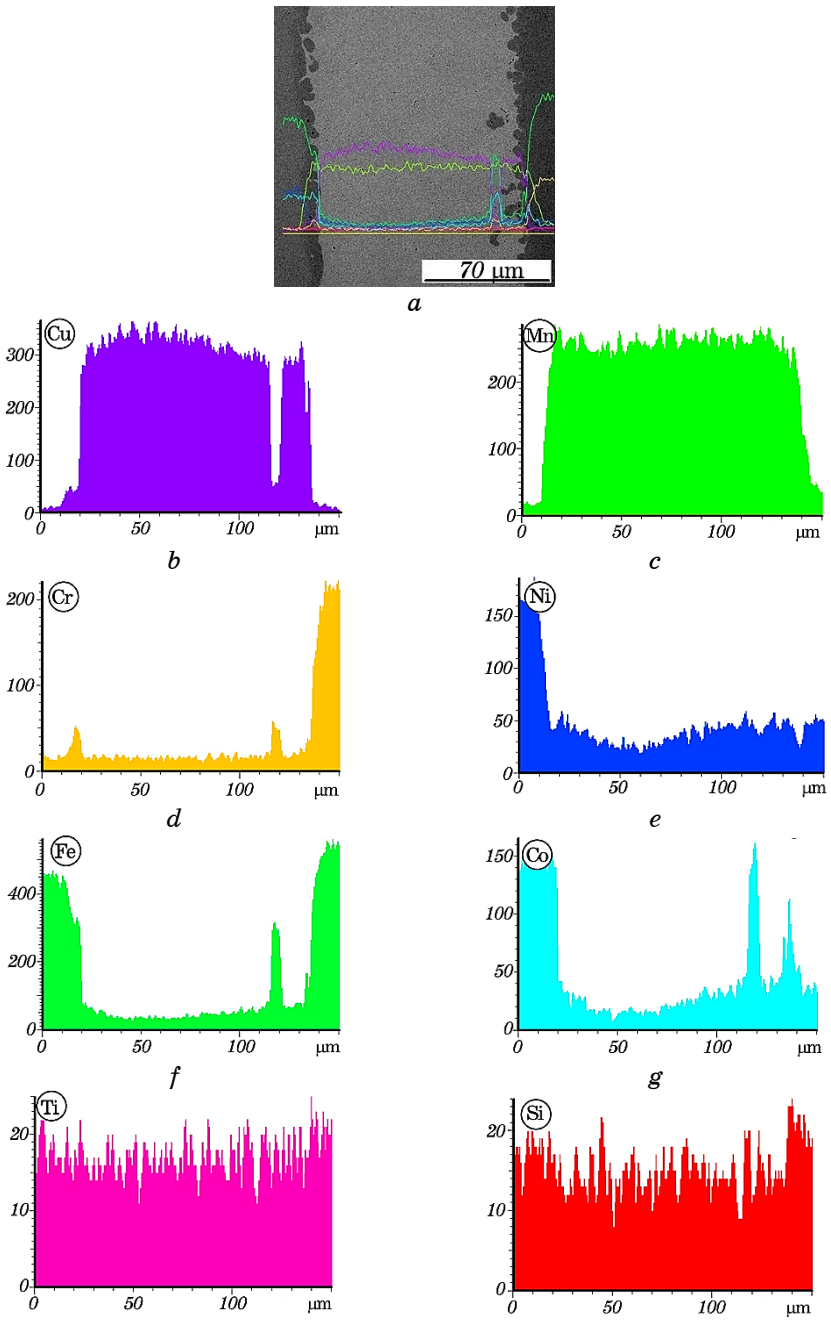

Fig. 4. Electronic image of the microstructure of the brazed joint (*a*) and the distribution of copper (*b*), manganese (*c*), chromium (*d*), nickel (*e*), iron (*f*), cobalt (*g*), titanium (*h*), and silicon (*i*).

Within the discrete dark grains, there is a noticeable increase in the concentration of iron, cobalt, and chromium, accompanied by a significant reduction in the amount of copper (Fig. 4).

The decrease in the amount of nickel, albeit to a lesser extent, is also notable during the scanning of this phase with a beam. Based on the findings from micro-x-ray spectral studies, it can be affirmed that active mutual diffusion processes occur between the components of the filler metal and the base metal during the formation of the structure of brazed joints. Specifically, iron, cobalt, nickel, chromium, and manganese exhibit such interactions. These processes are influenced by factors including the heating temperature, non-equilibrium conditions of crystallization of the brazing filler metal, and the chemical composition of both the base metal and filler metal.

Consequently, a concentration gradient emerges at the interface between the filler metal and the base metal.

Drawing upon the aforementioned results, a schematic representation of the metal structure formation of the brazed seam can be proposed (Fig. 5). This representation elucidates a significant transformation in the chemical composition of the original filler metal during

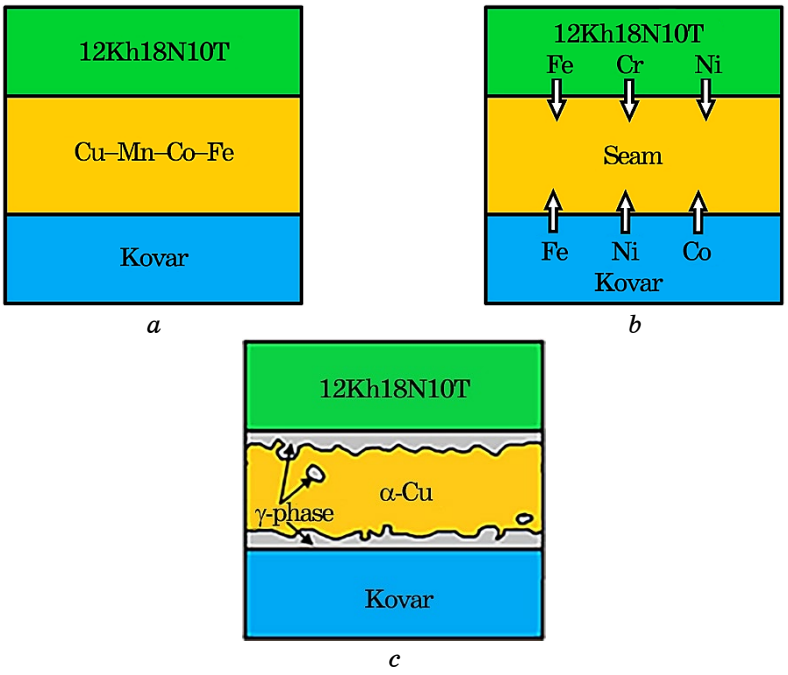

Fig. 5. Scheme of the formation of dissimilar Kovar joints with stainless steel with a gap of 100–50 μm: in the initial state (*a*); during heating (*b*) and after crystallization of the brazed seam (*c*).

TABLE 4. Chemical composition of separate phases in the Kovar–stainless steel brazed seam by 50 μm brazing gap.

No. spectrum	Chemical elements, wt. %							
	Si	Ti	Cr	Mn	Fe	Co	Ni	Cu
1	0.50	0.00	18.02	1.26	71.27	0.00	8.94	0.00
2	0.00	0.00	3.46	29.58	36.80	18.41	3.23	8.51
3	0.00	0.00	3.38	25.95	37.13	17.91	5.61	10.02
4	0.00	0.00	0.14	24.87	1.25	1.24	4.27	68.22
5	0.18	0.00	2.44	29.00	36.95	18.49	4.68	8.25
6	0.19	0.00	0.07	0.55	53.07	17.87	28.25	0.00

high-temperature brazing. This transformation contributes to the formation, alongside the solid solution (copper-based), of an iron-based phase manifested in the form of discrete single grains against a solid solution background.

Reducing the brazing gap size from 100 to 50 μm does not affect the morphology of the seam, but only leads to a decrease in its width (Fig. 6).

Similar to the previous sample, its structure is constituted by a copper–manganese solid solution, albeit with a slight reduction in its proportion compared to the previous sample, accounting for 82.25% of the total seam area. The concentration of iron in this solid solution remains consistent with the measurements of the previous sample, approximately at ≅ 1.25% (Fig. 6, Table 4, spectrum 4).

Notably, the proportion of the γ-phase ($Fe_xMn_yCo_z$)*Me* in the seam increases by approximately 4%, reaching 17.75%. This phase is predominantly observed near the interface of the filler metal with the base metal (Fig. 6, Table 4, spectrum No. 2 and No. 5).

Reducing the gap size to 20 μm during the brazing of dissimilar Ko-

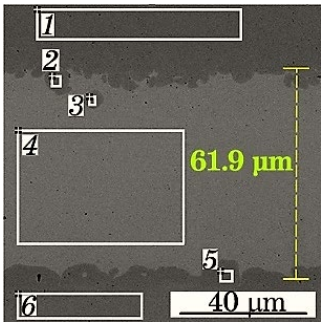

Fig. 6. Microstructure of a dissimilar brazed joint Kovar–stainless steel with the gap of 50 μm.

TABLE 5. Chemical composition of separate phases in the Kovar–stainless steel brazed seam by 20 μm brazing gap.

No. spectrum	Chemical elements, wt. %							
	Si	Ti	Cr	Mn	Fe	Co	Ni	Cu
1	0.25	0.00	5.15	20.25	46.13	11.25	9.46	7.52
2	0.00	0.00	0.74	17.68	6.39	1.71	7.49	65.99
3	0.33	0.19	9.85	16.28	53.58	7.43	8.00	4.34
4	0.21	0.00	4.94	20.34	46.18	10.56	9.63	8.13
5	0.16	0.00	0.23	0.36	54.08	17.68	27.49	0.00
6	0.47	0.23	17.81	1.31	70.59	0.44	8.89	0.26

var-stainless steel joints results in not only a decrease in the width of the brazed joint but also induces notable morphological changes in the structure during the crystallization of the brazed seam metal (Fig. 7).

Based on the research findings, there is a notable reduction in the amount of Cu–Mn solid solution in the brazed seam, accounting for only 9.10% of the total seam area. Additionally, data from local micro-x-ray spectral analysis reveal significant disparities in the chemical composition of separate phases compared to previous samples. Specifically, the concentration of iron in the solid solution increases to approximately ≅ 6.39% when the brazing gap size is reduced to 20 μm (Fig. 7 and Table 5, spectrum 2).

The concentration of iron in the γ-phase grains $(Fe_xMn_yCo_z)Me$ also escalates to 46.13–53.58%, concurrently with an increase in cobalt concentration to 7.43–11.25% (as per point local micro-x-ray spectral analysis data). Examining the obtained microstructures reveals that in

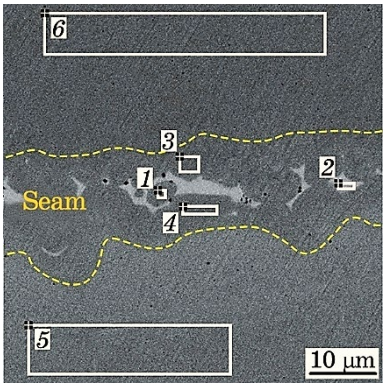

Fig. 7. Microstructure of the brazed seam of dissimilar Kovar–stainless steel joint by gap of 20 μm.

certain regions of the seam, these phase grains crystallize so closely together that they appear to amalgamate into conglomerates at the interphase boundary between the liquid filler metal and solid base metal, forming a continuous layer on the sides of both base materials: Kovar and stainless steel. It is evident that such features in the formation of the brazed seam structure can be attributed to the reduction in gap size. The vigorous interaction of the molten filler metal Cu–Mn–Co–Fe with the solid base metal during the brazing process also plays a role. Additionally, the resultant mutual diffusion processes at the filler metal-base metal interface contribute to this. These processes commence from the initial moments of the appearance of the liquid phase of the brazing filler metal [22].

Analysis of the obtained results regarding the local chemical composition of distinct phases in the brazed seam reveals (Fig. 8, *a*) that a decrease in the size of the brazing gap correlates with an increase in iron concentration in the γ-phase $(Fe_xMn_yCo_z)Me$, alongside a simultaneous reduction in manganese and cobalt content.

The reduction in gap size has minimal effect on the chemical composition of the Cu–Mn solid solution. However, it does result in a slight synchronous increase in the concentrations of Fe and Ni (Fig. 8, *b*).

It is important to note that despite the base metal remaining in the solid state during brazing, the structure and chemical composition of both the initial filler metal and the metal of the seam undergo significant disruption. Based on the results, it is possible to elucidate the underlying structural mechanism for the formation of the brazed seam. According to the chemical composition of the formed phases, the primary phase is the γ-phase $(Fe_xMn_zCo_y)Me$, as it can be associated with a higher temperature phase (Fig. 9, *a*, *b*) [23]. The secondary phase is a

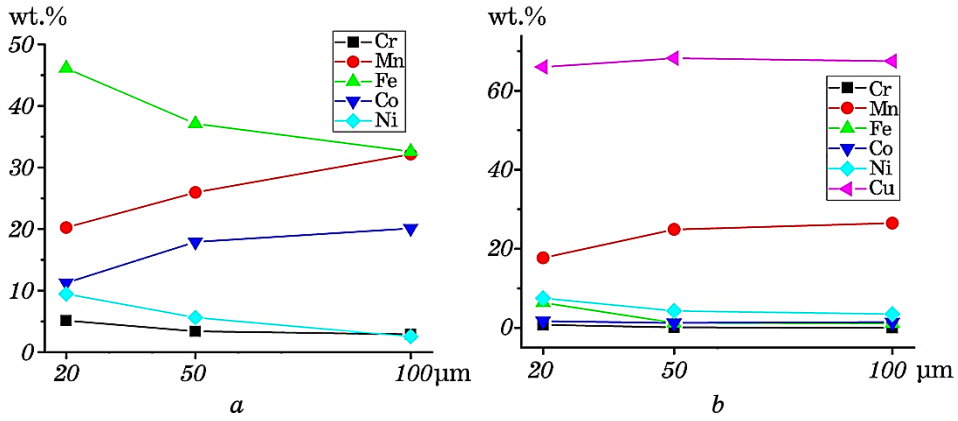

Fig. 8. Concentration of chemical elements in the γ-phase $(Fe_xMn_zCo_y)Me$ (*a*) and α-Cu solid solution (*b*) in the location depending on the size brazing gap.

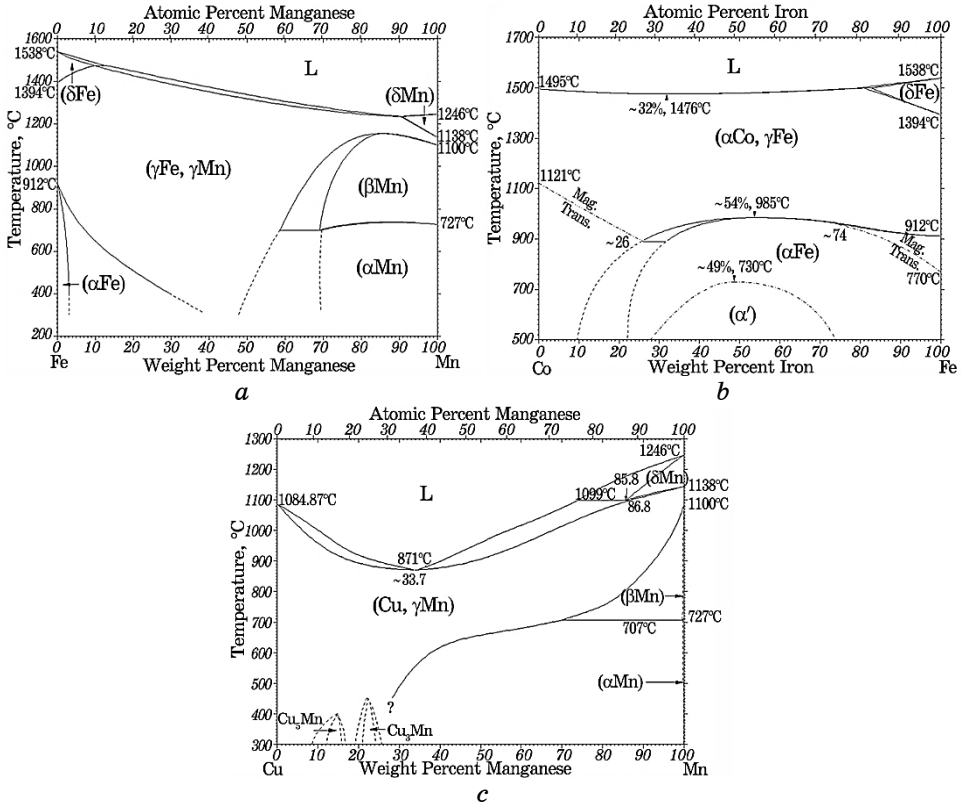

Fig. 9. Binary diagram Fe–Mn (*a*), Fe–Co (*b*), Cu–Mn (*c*).

copper-manganese solid solution, which fills the gap and crystallizes at a later stage (Fig. 9, *c*).

Furthermore, the findings from this study have demonstrated that the structure and morphological characteristics of the metal seams in brazed dissimilar joints between Kovar and stainless steel, utilizing Cu–Mn–Co–Fe filler metal, primarily hinge upon the width of the brazing gap size, thereby influencing diffusion processes. It has been established that the presence of $(Fe_xMn_yCo_z)Me$ is primarily dictated by the size of the brazing gap. Concurrently, empirical evidence has confirmed that an increase in gap size adversely influences the mechanical properties of brazed joints (Table 6), which can be attributed to the aforementioned structural attributes of brazed seams.

The brazed samples obtained with a minimum brazing gap of 20 μm exhibit maximum strength (600 MPa), with their failure occurring predominantly on the main metal—stainless steel, accompanied by minor plastic deformation. This observation underscores that the strength of a dissimilar joint obtained through brazing surpasses that of stainless

TABLE 6. Strength of brazed joints Kovar–stainless steel depending on the gap size (at 20°C).

Filler metal	Brazing gap size, μm	τ_s, MPa	σ_b, MPa	Fracture site
Cu–Mn–Co–2.5Fe	20	–	580–635	12Kh18N10T
	50	498–505	–	seam
	100	408–459	–	seam

steel subsequent to undergoing a high-temperature vacuum brazing cycle. Based on the obtained data, it is evident that the size of the brazing gap influences the morphology of the seam, the chemical composition of its separate phases, and the mechanical properties of brazed joints. The results of the conducted investigations validate the correlation between the structural attributes of brazed seams and their strength.

It is noteworthy that the trend of enhancing the mechanical properties of brazed joints with a reduction in gap size is also evident when brazing other materials (Fig. 10), such as 316 L steel utilizing BNi-2 (Ni620) filler metal [15].

This phenomenon can be attributed to the peculiarities of the microstructure following the crystallization of the brazed seam metal.

At gaps exceeding 50–60 microns, the central zone of the seam experiences the formation of brittle phases. Consequently, during mechanical tests, the failure of brazed samples is observed within these phases. Conversely, as the gap size decreases, the morphology of the brazed seams undergoes significant alterations, with the absence of brittle phases in the seams. Instead, failure occurs along the interphase boundary of the base metal and filler metal in the region where a solid solution forms [15].

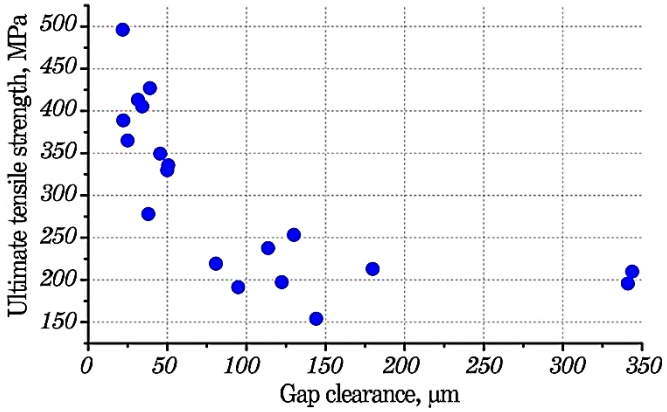

Fig. 10. Dependence of strength on gap size for BNi-2 [15].

4. CONCLUSION

Metallographic studies of dissimilar Kovar–stainless steel brazed joints confirmed the formation of a two-phase structure comprising of α-Cu solid solution (based on the Cu–Mn system) and grains of the γ-phase ($Fe_xMn_yCo_z$)*Me*. The volume ratio of these phases varies depending on the gap size. Decreasing the gap size from 100 to 20 μm results in a decrease in the solid solution amount from 86.83% to 9.10%, accompanied by a simultaneous increase in the γ-phase amount from 13.17 to 90.90%.

Reduction of the brazing gap size from 100 to 20 μm leads to an increase in iron concentration in the γ-phase from 32.58 to 46.13%, with a simultaneous decrease in manganese content from 32.16 to 20.25%, respectively. In the Cu–Mn solid solution, diminishing gap size causes a slight increase in iron amount from 1.12 to 6.39%.

Mechanical testing results indicate that reducing the brazing gap size from 100 to 50 μm enhances the shear strength of brazed joints from 408–459 to 498–505 MPa. Further reduction of the gap size to 20 μm boosts strength (up to 600 MPa), with sample failure occurring predominantly on the main metal—stainless steel with minor plastic deformation. This behaviour can be attributed to the structural characteristics of the brazed joints, notably the significant presence of the γ-phase (90.90%).

REFERENCES

1. G. J. Qiao, H. J. Wang, J. Q. Gao, and Z. H. Jin, *Mater. Sci. Forum*, **486–487**: 481 (2005).
2. Y. J. Fang, X. S. Jiang, D. F. Mo, T. F Song, Z. Y. Shao, D. G. Zhu, M. H. Zhu, and Z. P. Luo, *Adv. Mater. Sci. Eng.*, **2018**: 1 (2018).
3. G. Xia, C. Chen, J. Jia, W. Huang, H. Liu, and Y. Long, *Weld. World*, **68**: 1427 (2024).
4. B. Ahn, *Metals.*, **11**, No. 7: 1037 (2021).
5. C. Xin, Y. Jiazhen, N. Li, W. Liu, J. Du, Y. Cao, and H. Shi, *Ceram. Int.*, **42**, No.11: 12586 (2016).
6. L. F. Rudenko and T. P. Govorun, *Alloy Steels and Alloys* (Sumy: Sumy State University: 2012) (in Ukrainian).
7. S. H. Baghjari, M. Gholambargani, and S. A. A. Akbari Mousavi, *Lasers Manuf. Mater. Process.*, **6**: 14 (2019).
8. M. M. A. Fadhali, S. J. Zainal, Y. Munajat, A. Jalil, and R. Rahman, *AIP Conf. Proc.*, **1217**: 147 (2010).
9. Yu. V. Kaletina, E. D. Efimova, and M. K. Romanov, *Materials Science and Heat Treatment of Metals*, **6**: 26 (2014) (in Russian).
10. J. Feng, M. Herrmann, A.-M. Reinecke, and A. Hurtado, *J. Exp. Theor. Anal.*, **2**, No. 1: 1 (2024).
11. T. Song, X. Jiang, Z. Shao, D. Mo, D. Zhu and M. Zhu, *Metals*, **6**, No. 11: 263 (2016).

12. T. A. Mai and A. C. Spowage, *Mater. Sci. Eng. A*, **374**, Nos. 1–2: 224 (2004).
13. G. V. Ermolaev, V. V. Kvasnitsky, V. F. Kvasnitsky, S. V. Maksymova, V. F. Khorunov, and V. V. Chigarov, *Payannya Metaliv* [Brazing Materials] (Mykolaiv: NUK: 2015) (in Ukrainian).
14. V. M. Radziievskyi, A. F. Budnyk, and V. B. Yuskaiev, *Metallurgy of High-Temperature Technology of Non-Separable Joints* (Sumy: Sumy State University: 2011) (in Ukrainian).
15. E. Hedin, *Proc. of the 7th Int. Brazing and Soldering Conf. (IBSC) (Apr. 15–18, 2018, New Orleans, USA)*, p. 155–160.
16. S. V. Maksymova, V. F. Khorunov, and V. V. Voronov, *The Paton Welding J.*, **3**: 28 (2013).
17. S. V. Maksymova, P. V. Kovalchuk, V. V. Voronov, and I. I. Datsiuk, *The Paton Welding J.*, **8**: 13 (2023).
18. M. M. Shyshkov, *Marochnyk Staley i Splaviv: Dovidnyk* [Brand of Steels and Alloys: Directory] (Donetsk: 2000) (in Ukrainian).
19. https://metallicheckiy-portal.ru/marki_metallov/stk/12X18H10T
20. https://www.hightempmetals.com/techdata/hitempKovardata.php#4
21. A. M. Zakharov, *Diagrammy Sostoyaniya Dvoinykh i Troinykh Sistem* [State Diagrams of Binary and Ternary Systems] (Moskva: Metallurgiya: 1990) (in Russian).
22. S. V. Maksymova, *Current Topics and Emerging Issues in Materials Sciences*, **2**: 14 (2023).
23. T. B. Massalski, *Binary Alloy Phase Diagrams* (Materials Park, Ohio: ASM International: 1990). In CD.